J|A|C|S
ARTICLES

Published on Web 11/11/2009

Analyzing the Molecular Weight Distribution in Supramolecular Polymers

Stephan A. Schmid,[†] Robert Abbel,[‡] Albertus P. H. Schenning,[‡] E. W. Meijer,[‡] Rint P. Sijbesma,[‡] and Laura M. Herz*[,†]

Clarendon Laboratory, Department of Physics, University of Oxford, Parks Road, Oxford, OX1 3PU, United Kingdom, and Laboratory of Macromolecular and Organic Chemistry, Eindhoven, University of Technology, P.O. Box 513, 5600 Eindhoven, The Netherlands

Received September 22, 2009; E-mail: l.herz@physics.ox.ac.uk

Abstract: We have investigated the formation process of supramolecular linear polymer chains and its influence on the resulting chain length distribution function. For this purpose, we explored the migration of excitation energy between oligofluorene units coupled together through quadruple hydrogen-bonding groups to form linear chains that are terminated by oligophenylene vinylene end-caps acting as energy traps. The energy transfer dynamics from the main chain to the chain end was monitored experimentally using time-resolved PL spectroscopy and compared to an equivalent Monte Carlo simulation incorporating information on the structure of the chains, the transition transfer rates, and various weight distribution trial functions. We find that the assumption of a Flory distribution of chain lengths leads to excellent agreement between experimental and simulated data for a wide range of end-cap concentrations. On the other hand, both a Poisson function and a simplified assumption of a monodisperse distribution significantly underestimate the presence of long chains in the ensemble. Our results therefore show that supramolecular polymerization is a steplike process equivalent to polycondensation reactions in linear covalent polymers. These findings emphasize that equal reactivity of the supramolecular building blocks leads to a dynamic growth process for the supramolecular chain involving all chain components at all times.

Introduction

Supramolecular self-assembly of molecules into complex architectures has been exploited by nature over the course of its evolution, facilitating, for example, the assembly of proteins[1] and photosynthetic reaction centers.[2] More recently, research has been directed at exploiting such processes to induce mesoscopic order in π-conjugated materials for applications in organic electronic devices.[3] Here, supramolecular π-conjugated assemblies offer to combine the mechanical flexibility of polymers[4,5] with the well-defined electronic properties of small oligomers.[6−8] Intermolecular interactions such as ionic or hydrogen bonding or solvophobic, solvophilic, and $\pi-\pi$ interactions between monomeric units can be tailored to generate desired supramolecular structures in solution, which may endure the casting process into solid films.[9−11] In the case of linear self-assembled structures, referred to as "supramolecular polymers", monomers are held together by noncovalent bonds, leading to a reversability of the polymerization process.

A remaining challenge in the area of supramolecular design and implementation is the lack of obtainable information on the size distribution present in an ensemble of such assemblies. For example, supramolecular polymers formed during a polycondensation process are unlikely to exhibit uniform lengths or weights and need to be characterized by a weight fraction distribution. For covalent synthetic processes such as polymerization reactions, on the other hand, characterization is comparatively simple, because an equilibration between linear chains of various lengths and cyclic products is established only during synthesis. Several chemical and physical methods are available to determine the ensemble-averaged molecular weight for a polymer sample, as, for example, osmotic measurements,[12,13] light scattering experiments, viscosity measurements, and ultracentrifugation.[14] Analyzing the distribution of linear and cyclic products can be achieved by isolation of the individual fractions of the polymeric ensemble, for instance, via fraction-

[†] University of Oxford.
[‡] Eindhoven University of Technology.

(1) Oosawa, F.; Asakura, S. *Thermodynamics of the Polymerization of Protein*; Academic Press: London, 1975.
(2) Deisenhofer, J.; Norris, J. R. *The Photosynthetic Reaction Center*; Academic Press: New York, 1993.
(3) Sirringhaus, H.; Brown, P. J.; Friend, R. H.; Nielsen, M. M.; Bechgaard, K.; Langeveld-Voss, B. M. W.; Spiering, A. J. H.; Janssen, R. A. J.; Meijer, E. W.; Herwig, P. *Nature* **1999**, *401*, 685–688.
(4) Yaliraki, S. N.; Silbey, R. J. *J. Chem. Phys.* **1996**, *104*, 1245.
(5) Woo, H. S.; Lhost, O.; Graham, S. C.; Bradley, D. D. C.; Friend, R. H.; Quatrocchi, C.; Breédas, J. L.; Schenk, R.; Müllen, K. *Synth. Met.* **1993**, *59*, 13.
(6) Maddux, T.; Li, W.; Yu, L. *J. Am. Chem. Soc.* **1997**, *119*, 844.
(7) Meier, H.; Stalmach, U.; Kolshorn, H. *Acta Polym.* **1997**, *48*, 379.
(8) Klaerner, G.; Miller, R. D. *Macromolecules* **1998**, *31*, 2007.
(9) Lehn, J.-M. *Proc. Natl. Acad. Sci. U.S.A.* **2002**, *99*, 4763.
(10) Jonkheijm, P.; Hoeben, F. J. M.; Kleppinger, R.; van Herrikhuyzen, J.; Schenning, A. P. H. J.; Meijer, E. W. *J. Am. Chem. Soc.* **2003**, *125*, 15941.
(11) Schenning, A. P. H. J.; Jonkheijm, P.; Hoeben, F. J. M.; Meskers, S. C. J.; Meijer, E. W.; Herz, L. M.; Daniel, C.; Silva, C.; Phillips, R. T.; Friend, R. H.; Beljonne, D.; Miura, A.; Zdanowska, M.; Uji-i, H.; Chen, Z. *Synth. Met.* **2004**, *147*, 43–48.
(12) Flory, P. J. *J. Am. Chem. Soc.* **1943**, *65*, 372.
(13) Krigbaum, W. R.; Flory, P. J. *J. Am. Chem. Soc.* **1953**, *75*, 1775.

 10.1021/ja9080452 © **2009 American Chemical Society**

ation or chromatographic methods.[15] Size exclusion chromatography (SEC)[16] represents a state-of-the-art technique to determine the weight fraction distribution of covalent polymers. However, the usage of these techniques to characterize supramolecular self-assembly processes is problematic, because here the polymerization process is reversible. The assembly is therefore in a free equilibrium with its components, which results in significant tailing of the distribution obtained from SEC, and well-defined peaks only appear in case of negligible assembly reversibility.[15,17] While SEC has led to reasonable results for the characterization of biomolecular[18−20] and stable synthetic complexes,[21−24] this cannot be expected for reversible linear polymers, as the molecular weight of the polymerization products is continuously redistributed during the chromatography. Thus, the experimental determination of the weight fraction distribution of reversible linear polymers still remains challenging.

In the study presented here, we have investigated the supramolecular polymerization process for a system of chain-building and stopping units coupled through reversible quadruple hydrogen bonds. Using time-resolved photoluminescence (PL) spectroscopy, we were able to measure the dynamics of energy transfer from the main-chain oligofluorene (OF) building blocks to the oligophenylenevinylene (OPV) end groups terminating the chain. The experimental data were subsequently compared to the output from a Monte Carlo simulation of exciton migration along the chains, which incorporated a number of different trial functions for potential chain lengths distributions. We find that this approach represents a highly powerful means of determining the present chain lengths distribution functions because the weighting of short- to long-decay components in the transient directly maps out the prevalence of short to long chains in the supramolecular ensemble, with fast energy tranfer components arising from short chains and long components from lifetime-limited exciton decays on long chains.

Comparison of the simulated PL transients with the experimental data shows excellent correspondence with the assumption of a Flory distribution of chain lengths, while a Poisson distribution is found to underestimate the presence of long chains in the ensemble. In addition, the assumption of a monodisperse ensemble, as suggested recently,[25] is found to provide a poor match between simulated and experimental PL transients. Our results demonstrate that the formation of supramolecular polymers from chain building and stopping units follows a step-polymerization reaction with equal reactivity of all supramolecular building blocks at any stage. "Growth" of the supramolecular chain is therefore a dynamic process involving all chain components at all times.

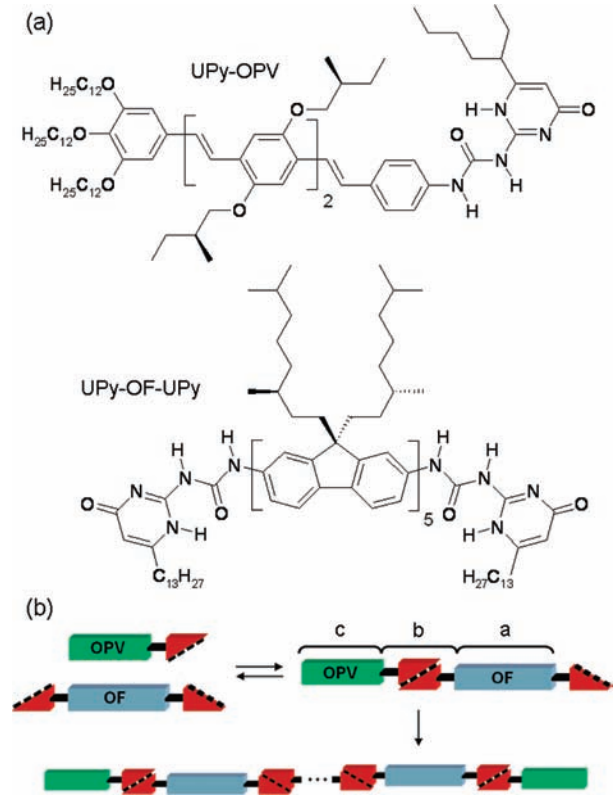

Figure 1. (a) Chemical structure of UPy-terminated oligo(*p*-phenylenevinylene) (UPy−OPV) and bis-UPy-terminated oligofluorene (UPy−OF−UPy), and (b) schematic representation of the self-assembly process into linear supramolecular polymers with geometric definitions of the structural parameters *a*, *b*, and *c* (see text).

The system under investigation is shown in Figure 1 and comprises blends of OF units bis-terminated with functional 2-ureido-4[1*H*]-pyrimidinone (UPy) groups (UPy−OF−UPy) and OPV units monoterminated with UPy (UPy−OPV). The synthesis and characterization of the compounds have already been described in detail in refs 26 and 27. Both chromophores have been explored for light emitting diodes and exhibit high fluoresence quantum yields.[28−30] The UPy group contains two hydrogen-donating and -accepting sites allowing the formation of self-complementary (DDAA) quadruple hydrogen bonds with high directionality.[31,32] Recent viscosity measurements and titration experiments indicate that in solution, bis-terminated UPy−OF−UPy units assemble into linear polymer-like structures, with monoterminated UPy−OPV acting as stoppers on either end of the chain (see Figure 1b).[26,32,33] Quadruple hydrogen-bonding groups are particularly suitable for the

(14) Flory, P. J. *Principles of Polymer Chemistry*; Cornell University Press: Ithaca, 1953.
(15) ten Cate, A. T.; Sijbesma, R. P. *Macromol. Rapid Commun.* **2002**, *23*, 1094.
(16) Strobl, G. *Physics of Polymers -Concepts for Understanding Their Structures and Behaviour*; Springer: Berlin, 2007.
(17) Kolotuchin, S. V.; Zimmerman, S. C. *J. Am. Chem. Soc.* **1998**, *120*, 9092.
(18) Stevens, F. J. *Biochemistry* **1986**, *25*, 981.
(19) Raffen, R.; Stevens, F. J. *Methods Enzymol.* **1999**, *309*, 318.
(20) Patapoff, T. W.; Mrsny, R. J.; Lee, W. A. *Anal. Biochem.* **1993**, *212*, 71.
(21) Whitesides, G. M.; Simanek, E. E.; Mathias, J. P.; Seto, C. T.; Chin, D. N.; Mammen, M.; Gordon, D. M. *Acc. Chem. Res.* **1995**, *28*, 37.
(22) Zimmerman, S. C.; Zeng, F.; Reichert, D. E. C.; Kolotuchin, S. V. *Science* **1996**, *271*, 1095.
(23) Corbin, P. S.; Lawless, L. J.; Li, Z.; Ma, Y.; Witmer, M. J.; Zimmermann, S. C. *Proc. Natl. Acad. Sci. U.S.A.* **2002**, *99*, 5099.
(24) Ma, Y.; Kolotuchin, S. V.; Zimmermann, S. C. *J. Am. Chem. Soc.* **2002**, *124*, 13757.
(25) Drain, C. M.; Shi, X.; Milic, T.; Nifiatis, F. *Chem. Commun.* **2001**, 287.
(26) Dudek, S. P.; Pouderoijen, M.; Abbel, R.; Schenning, A. P. H. J.; Meijer, E. W. *J. Am. Chem. Soc.* **2005**, *127*, 11763.
(27) Abbel, R.; Grenier, C.; Pouderoijen, M. J.; Stouwdam, J. W.; Leclére, P. E. L. G.; Sijbesma, R. P.; Meijer, E. W.; Schenning, A. P. H. J. *J. Am. Chem. Soc.* **2009**, *131*, 833.
(28) Jo, J.; Chi, C.; Höger, S.; Wegner, G.; Yoon, D. Y. *Chem.-Eur. J.* **2004**, *10*, 2681.
(29) Lee, S. H.; Tsutsui, T. *Thin Solid Films* **2000**, *363*, 76.
(30) Liu, B.; Wang, S.; Bazan, G. C.; Mikhailovsky, A. *J. Am. Chem. Soc.* **2003**, *125*, 13306.
(31) Sijbesma, R. P.; Meijer, E. W. *Chem. Commun.* **2003**, 5.
(32) Sijbesma, R. P.; Beijer, F. H.; Brunsveld, L.; Folmer, B. J. B.; Hirschberg, J. H. K. K.; Lange, R. F. M.; Lowe, J. K. L.; Meijer, E. W. *Science* **1997**, *278*, 1601.

generation of supramolecular polymers as they offer high interaction strength ($K_a \approx 10^7$ M^{-1}) and thus a large degree of polymerization.[34] Specifically, for the solvent used in the present study ($CHCl_3$), the lifetime of the UPy−UPy hydrogen bond is of the order of 0.1 s,[35] meaning that the composition of the supramolecular chains remains static during the time scale of exciton migration along the chains.

Experimental Results

Measurement Details. All measurements were taken for blends of UPy−OF−UPy and UPy−OPV molecules dissolved in $CHCl_3$ at concentrations of 4×10^{-4}. Time-resolved photoluminescence (PL) measurements were conducted using an up-conversion setup that has already been described in detail elsewhere.[36] Solutions held in quartz cuvettes were excited at a photon energy of 3.30 eV and fluence of 3 nJ cm^{-2} with frequency-doubled pulses of 100 fs duration originating from a mode-locked Ti:Sapphire oscillator. The emerging photoluminescence was collected by a pair of off-axis parabolic mirrors and focused onto a β-barium-borate (BBO) crystal mounted on a rotation stage to allow tuning of the phase-matching angle. An intense vertically polarized gate beam (photon energy 1.65 eV) arriving at the BBO crystal at adjustable time delays was used to up-convert the PL at given times after excitation. The resulting sum-frequency photons were collected, dispersed in a monochromator (Jobin Ivon Triax 190), and detected by a liquid-nitrogen cooled CCD. Only the vertical polarization component of the PL was up-converted in this setup; therefore, either the parallel or the perpendicular luminescence polarizations with respect to the excitation polarization was selected by changing the polarization of the excitation beam through rotation of a half-wave plate and a Glan-Thompson polarizer. The temporal resolution of the system was determined to be ~800 fs. Both steady-state PL measurements were taken by removing the BBO crystal and replacing it with a linear Glan−Thompson polarizer. Absorption spectra were taken with a commercial spectrophotometer. All measurements were conducted at room temperature and corrected for spectral response of the apparatus.

Absorption and Emission Spectra. Figure 2 shows the optical absorption and time-integrated PL spectra of the UPy−OF−UPy and UPy−OPV solutions. The molar extinction coefficient is high for both compounds (peak values of ~185 000 L mol^{-1} cm^{-1} at 3.30 eV and ~83 000 L mol^{-1} cm^{-1} at 2.85 eV for UPy−OF−UPy and UPy−OPV, respectively) in agreement with previous studies.[26] For efficient transfer of excitation energy, spectral overlap between donor emission and acceptor absorption is required.[37−39] The emission from UPy−OF−UPy and the absorption of UPy−OPV show strong overlap, which gives promise to highly efficient heterotransfer of excitons from UPy−OF−UPy to UPy−OPV. In addition, less efficient, but still significant homotransfer between neighboring UPy−OF−UPy molecules can be expected, because absorption and emission from the oligofluorene show some spectral overlap. Following excitation of UPy−OF−UPy units, exciton migration along UPy−OF−UPy units of the same chain and direct excitation transfer to the UPy−OPV chain ends will therefore form two competing processes. However, once an excitation reaches the chain end, it is expected to become localized, as there is insignificant spectral overlap between UPy−OPV emission and UPy−OF−UPy absorption.

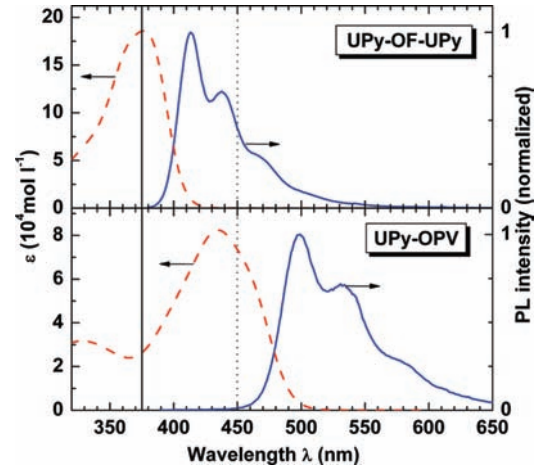

Figure 2. Absorption (red, dashed line) and steady-state photoluminescence spectra (blue, solid line) for UPy−OF−UPy and UPy−OPV at 4×10^{-4} M in $CHCl_3$, with ε being the molar extinction coefficient. The wavelengths of excitation (solid) and signal detection (dotted) are indicated as vertical lines.

Absorption spectra of both species exhibit considerable broadening. In contrast, the photoluminescence spectra show a clearly resolvable vibronic progression, with a spacing of approximately 0.18 eV between the vibronic peaks associated to the C=C stretching mode.[40] The peaks in the absorption and emission spectra of both species are energetically displaced with respect to each other by a significant Stokes shifts (≤0.2 eV). For conjugated polymers, a lack of mirror symmetry between absorption and emission spectra has generally been attributed to the presence of an inhomogeneous distribution of chromophore types.[41−43] In this case, creation of an excited state within the inhomogeneously broadened density of states is followed by energetic relaxation toward lower-energy sites, leading to spectral narrowing of the emission and an additional Stokes shift. However, for short oligomers such as those investigated here, inhomogeneous broadening due to conformational disorder can in general be neglected, as these tend to have well-defined sizes and uniform conjugation lengths. Instead, the lack of mirror symmetry has been attributed to low-energy vibrational modes being stiffer in the excited state than in the ground state, making the associated spectral broadening significantly more pronounced in absorption than in emission.[44,45]

Excitation Energy Transfer Dynamics. Figure 3 shows the temporal evolution of the PL intensity emitted from UPy−OF−UPy in blend solutions of different mixing ratio x. The emission from pure UPy−OF−UPy solutions ($x = 0$) displays an almost monoexponential ($\tau \approx 305$ ps) decay, with a minor, slightly faster component decaying within the first few tens of picoseconds. As reported in recent studies on oligofluorenes, this small deviation may be owed to torsional relaxation processes of the UPy−OF−UPy molecules upon photoexcitation.[46] However, upon addition of UPy−OPV, the PL originating from UPy−OF−UPy decays faster

(33) Ligthart, G. B. W. L.; Ohkawa, H. P.; Sijbesma, R.; Meijer, E. W. *J. Am. Chem. Soc.* **2005**, *127*, 810.
(34) Brunsveld, L.; Folmer, B. J. B.; Meijer, E. W.; Sijbesma, R. *Chem. Rev.* **2001**, *101*, 4071.
(35) Söntjens, S. H. M.; Sijbesma, R. P.; van Genderen, M. H. P.; Meijer, E. W. *J. Am. Chem. Soc.* **2000**, *122*, 7487.
(36) Chang, M. H.; Hoffmann, M.; Anderson, H. L.; Herz, L. M. *J. Am. Chem. Soc.* **2008**, *130*, 10171.
(37) Förster, T. *Discuss. Faraday Soc.* **1959**, *27*, 7.
(38) Förster, T. Delocalized excitation and excitation transfer. In *Modern Quantum Chemistry*; Sinanoglu, O., Ed.; Academic Press: London, 1965.
(39) Scholes, G. D. *Annu. Rev. Phys. Chem.* **2003**, *54*, 57–87.
(40) Cornil, J.; Beljonne, D.; Heller, C.; Campbell, I.; Laurich, B.; Smith, D.; Bradley, D.; Müllen, K.; Brédas, J. *Chem. Phys. Lett.* **1997**, *278*, 139.
(41) Movaghar, B.; Grünewald, M.; Ries, B.; Bässler, H.; Würtz, D. *Phys. Rev. B* **1986**, *33*, 5545.
(42) Rauscher, U.; Bässler, H.; Bradley, D. D. C.; Hennecke, M. *Phys. Rev. B* **1990**, *42*, 9830.
(43) Richert, R.; Bässler, H. *Chem. Phys. Lett.* **1985**, *118*, 235.
(44) Karabunarliev, S.; Bittner, E. R.; Baumgarten, M. *J. Chem. Phys.* **2001**, *114*, 5863.
(45) Karabunarliev, S.; Baumgarten, M.; Bittner, E. R.; Müllen, K. *J. Chem. Phys.* **2000**, *113*, 11372.

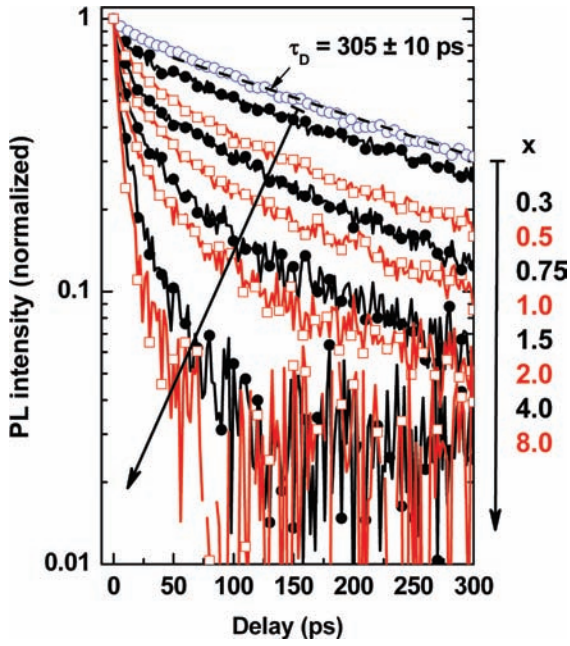

Figure 3. Time-resolved photoluminescence from blends of UPy−OF−UPy and UPy−OPV in $CHCl_3$ for various mixing ratios x (see text), detected at 450 nm (solid black and red lines). For the decay curve of the pure UPy−OF−UPy solution (blue circles), a monoexponential fit to the data from 50 ps onward (black, dashed line) is displayed together with the extracted lifetime τ.

with increasing mixing ratio, in accordance with increasing energy transfer to the chain ends. As merely luminescence emerging from UPy−OF−UPy is detected, energy transfer to UPy−OPV molecules represents an additional de-excitation channel for UPy−OF−UPy beside radiative recombination. With increasing concentration of UPy−OPV, the average chain length is decreasing, shortening the average transfer distance for heterotransfer and leading to the observed faster PL intensity decays. The donor decay dynamics for the blend solutions are also clearly nonexponential, displaying a fast component within the first ∼50 ps whose contribution increases and whose decay time decreases with increasing x, while at later times ($t > 100$ ps) the decay is comparable to that of the pure UPy−OF−UPy solution. Such variations in energy transfer rates can be attributed to the inhomogeneous distribution of transfer distances in the system.[47] At early times, the strong PL decay quenching is owed to energy transfer between pairs of UPy−OF−UPy and UPy−OPV molecules closely located to one another. At later times, the PL mainly emerges from the recombination of excitons residing on UPy−OF−UPy molecules that are spatially well separated from accepting UPy−OPV molecules. Thus, quenching of the PL through energy transfer is unlikely at later times, and the PL decay is governed by the natural lifetime of the UPy−OF−UPy excited state.

Time-Resolved PL Anisotropy. Figure 4 shows the PL polarization anisotropy measured for a pure UPy−OF−UP solution ($x = 0$), which remains constant at ∼0.4 over the complete lifetime of the excited state. Exciton transfer between adjacent UPy−OF−UPy units is therefore clearly not associated with a rotation of the excitonic dipole moment, which implies that the transition dipole moments of the donor and the acceptor site are oriented parallel to each other.[48,49] These results indicate that the entire supramolecular chain has a fairly straight geometry, with a bonding angle between

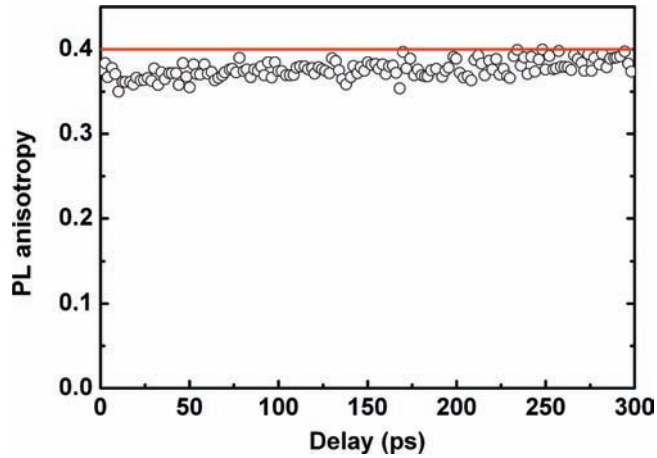

Figure 4. Time-resolved photoluminescence polarization anisotropy for UPy−OF−UPy solution in $CHCl_3$, detected at 450 nm. The red line indicates the value of 0.4 expected for a randomly oriented ensemble of molecules with well-defined absorption and emission dipole moments that are mutually parallel.

adjacent repeat units of ∼180°. Cyclization processes,[15] in which ring structures are formed by direct connexion between the two ends of an existing polymer strand, can be of importance at high concentrations of molecules functionalized with hydrogen-bonding groups on both ends.[27] However, for the supramolecular chains terminated with monofunctionalized end stoppers that are investigated here, such processes are shown to be absent. This finding is further supported by ^{1}H NMR measurements on diluted solutions of UPy-terminated bifunctional oligofluorenes of various molecular weights, which indicated the absence of cyclic structures at detectable concentrations.[26]

Simulation of Excitation Migration

Chain Structure and Model Parameters. To describe the structure of the supramolecular chains shown in Figure 1b, we introduce three parameters: the lengths of the OF- and the OPV-backbone, defined as a and c, and the extension of the UPy−UPy hydrogen bridge, defined as b. Because the oligomers are short and fairly rigid, a and c correspond to the conjugation lengths of UPy−OF−UPy and UPy−OPV, respectively. Values for the structural parameters were determined through molecular modeling using commercial structure calculation software (Gaussian 03) based on the semiempirical Austin Model 1[50] and a Polak−Ribiere algorithm to find the minima of the molecular potentials. To reduce the computational effort, simple methyl groups were substituted as side-chains as these have little influence on the extension of the π-conjugation. To increase accuracy, the quadruple hydrogen bonds between two adjacent UPy-groups were set to fixed bond lengths of ∼3 Å, as determined from single-crystal X-ray diffraction measurements on diaminotriazine and diaminopyrimidines derivatives that exhibit equivalent self-complementary arrays of hydrogen bonds.[51] The resulting values for a, b, and c are given in Table 1. In addition, the modeling confirms that assemblies of the oligomers form a straight line without observable chain bending, in agreement with the observed absence of anisotropy depolarization in the emission from these chains.

(46) Hintschich, S. I.; Dias, F. B.; Monkman, A. P. *Phys. Rev. B* **2006**, *74*, 045210.
(47) Herz, L. M.; Silva, C.; Grimsdale, A. C.; Müllen, K.; Phillips, R. T. *Phys. Rev. B* **2004**, *70*, 165207.
(48) Valeur, B. *Molecular Fluorescence: Principles and Applications*; Wiley−VCH: Weinheim, 2002.
(49) Schmid, S. A.; Yim, K. H.; Chang, M. H.; Zheng, Z.; Huck, W. T. S.; Friend, R. H.; Kim, J. S.; Herz, L. M. *Phys. Rev. B* **2008**, *77*, 115338.
(50) Dewar, M. J. S.; Zoebisch, E. G.; Healy, E. F.; Stewart, J. J. P. *J. Am. Chem. Soc.* **1985**, *107*, 3902.
(51) Beijer, F. H.; Kooijman, H.; Spek, A. L.; Sijbesma, R. P.; Meijer, E. W. *Angew. Chem., Int. Ed.* **1998**, *37*, 75.

Table 1. Values for the Model Parameters *a*, *b*, and *c* As Defined in Figure 1, Obtained from Molecular Modeling Calculations As Described in the Text

parameter	value
a [Å]	40 ± 1
b [Å]	11 ± 1
c [Å]	23 ± 1

Hopping Rates. Excitation energy transfer processes in conjugated materials fall between the two limiting cases of strong and weak electronic coupling. Here, strong coupling describes the scenario for which the electronic coupling strengths U_{DA} between a donor D and an acceptor A is significantly larger than the vibrational relaxation energy lost after geometric rearrangement in the excited state. In this case, an excited state may become fully or partly delocalized over the entire donor−acceptor system.[52−54] However, the supramolecular linear architecture of the UPy−OF−UPy chains places individual chromophores in insufficiently close proximity for such delocalization effects to apply. Instead, we have therefore modeled these processes within the weak coupling regime, for which the excited UPy−OF−UPy chromophore is expected to have geometrically relaxed to its equilibrium lattice configuration prior to energy transfer. In this limit, the migration of excitation energy through the ensemble of chromophores can be considered as a Markovian sequence of incoherent hopping steps, each of which being an elementary energy transfer process between a donor and an acceptor site.[55,56] The rate for energy transfer from an excited donor to an acceptor in its ground state may then be calculated using Fermi's Golden Rule as[39,57]

$$k_{DA} = \frac{2\pi}{\hbar}|U_{DA}|^2 J^*_{DA} \tag{1}$$

where J^*_{DA} denotes the spectral overlap between donor emission and acceptor absorption spectra normalized on an energy scale.

The most commonly used approach toward calculating the energy transfer rate is based on Förster's classical point-dipole approximation, which yields[37,38,58,59]

$$k_{DA} = \frac{1}{\tau_D}\left(\frac{R_0}{R_{DA}}\right)^6 \tag{2}$$

with

$$R_0 = \left[\frac{9000 \ln 10}{128\pi^5}\frac{\kappa^2 \Phi_D}{n^4 N} J_{DA}\right]^{1/6} \tag{3}$$

being the Förster radius.[37,38,58,59] R_0 denotes the donor−acceptor separation at which excitation transfer is as likely to occur as de-excitation of the donor by all other relaxation processes. Here, τ_D is the lifetime of the donor excitation in the absence of acceptors, n is the refractive index of the solvent, N is Avogadro's number, and Φ_D is the PL quantum yield of the donor. The spectral overlap factor J_{DA} is calculated as the overlap between the molar decadic extinction coefficient of the acceptor $\varepsilon_A(\nu)$ and the fraction of photons $f_D(\nu)$ with wavenumber ν emitted per unit wavenumber from the donor in the absence of acceptors,

$$J_{DA} = \int f_D(\nu)\varepsilon_A(\nu)\frac{d\nu}{\nu^4} \tag{4}$$

κ is the orientation parameter and describes the dependence of the transfer rate on the relative orientation of the two transition dipole moments and their displacement vector. For the supramolecular chains considered here, donor and acceptor adopt a parallel in-line geometry for which $\kappa^2 = 4$.[48]

However, for intermolecular separations that are comparable to the chromophore lengths, the point dipole model is no longer an appropriate choice, as it averages away the local character of the chromophore.[60,61] The line-dipole model, as presented by Grage et al., represents a refinement of Förster's model and takes into account the delocalization of the exciton on the chromophores by subdividing the transition dipole moment M into a set of subdipoles M_i, each of which is weighted according to the exciton wave function $\psi(i)$.[62] Within this approximation, the excited state of the donor and the ground state of the acceptor are generally assumed to be equally delocalized.[63−65] By approximating the shape of the molecule as a finite, one-dimensional periodic chain, $\psi(i)$ can be derived as

$$\psi(i) = \frac{\sin[\pi i/(L+1)]}{\sum_a^L \sin[\pi a/(L+1)]} \tag{5}$$

where L is the number of subdipoles. The total electronic donor−acceptor coupling is then calculated as the sum of the interactions between each pair of subdipoles. In analogy to the procedure for the point-dipole model, the transfer rate is then determined to be

$$k_{DA} = \frac{1}{\tau_D}(R_0)^6\left[\sum_{i,j}^{L}\frac{\psi(i)\psi(j)}{R^3_{DA^{ij}}}\right]^2 \tag{6}$$

where $R_{DA^{ij}}$ denotes the center-to-center distance between the ith subdipole on the donor and the jth one on the acceptor.

However, as we have recently shown, the line-dipole model's assumption of equally delocalized donor and acceptor wave functions leads to inaccurate predictions of the electronic transfer rates as it fails to account for excitonic self-localization.[66] Strong electron−phonon coupling in conjugated materials is expected to cause an ultrafast self-localization of the excitonic state upon vibrational relaxation.[67] For example, the relaxed excited state

(52) Clark, J.; Silva, C.; Friend, R. H.; Spano, F. C. *Phys. Rev. Lett.* **2007**, *98*, 206406.
(53) Chang, M. H.; Hoeben, F. J. M.; Jonkheijm, P.; Schenning, A. P. H. J.; Meijer, E. W.; Silva, C.; Herz, L. M. *Chem. Phys. Lett.* **2006**, *418*, 196.
(54) Chang, M. H.; Frampton, M. J.; Anderson, H. L.; Herz, L. M. *Phys. Rev. Lett.* **2007**, *98*, 027402.
(55) Bässler, H. Transport and relaxation of excitations in random organic solids: Monte Carlo simulation and experiment. In *Hopping and Related Phenomena*; Fritzsche, H., Polak, M., Eds.; World Scientific: River Edge, NJ, 1990.
(56) Hennebicq, E.; Pourtois, G.; Scholes, G. D.; Herz, L. M.; Russell, D. M.; Silva, C.; Setayesh, S.; Grimsdale, A. C.; Müllen, K.; Brédas, J. L.; Beljonne, D. *J. Am. Chem. Soc.* **2005**, *127*, 4744.
(57) May, V.; Kühn, O. *Charge and Energy Transfer Dynamics in Molecular Systems*, 2nd ed.; Wiley−VCH: Weinheim, 2004.
(58) Förster, T. *Fluoreszenz Organischer Verbindungen*; Valdenhoeck and Ruprecht: Göttingen, 1951.
(59) Dexter, D. L. *J. Chem. Phys.* **1953**, *21*, 836.
(60) Krueger, B. R.; Scholes, G. D.; Fleming, G. R. *J. Phys. Chem. B* **1998**, *102*, 5378.
(61) Beljonne, D.; Pourtois, G.; Silva, C.; Hennebicq, E.; Herz, L. M.; Friend, R. H.; Scholes, G. D.; Setayesh, S.; Müllen, K.; Brédas, J. L. *Proc. Natl. Acad. Sci. U.S.A.* **2002**, *99*, 10982.
(62) Grage, M. M.-L.; Pullerits, T.; Ruseckas, A.; Theander, M.; Inganäs, O.; Sundström, V. *Chem. Phys. Lett.* **2001**, *339*, 96.
(63) Beenken, W. J. D.; Pullerits, T. *J. Phys. Chem. B* **2004**, *108*, 6164.
(64) Westenhoff, S.; Daniel, C.; Friend, R. H.; Silva, C.; Sundström, V.; Yartsev, A. *J. Chem. Phys.* **2005**, *122*, 094903.
(65) Westenhoff, S.; Beenken, W. J. D.; Friend, R. H.; Greenham, N. C.; Yartsev, A.; Sundström, V. *Phys. Rev. Lett.* **2006**, *97*, 166804.
(66) Schmid, S. A.; Abbel, R.; Schenning, A. P. H. J.; Meijer, E. W.; Herz, L. M. *Phys. Rev. Lett.*, submitted.

Table 2. Experimentally Obtained Input Parameters for the MC Simulations[a]

parameter	value
R_{HOM} [Å]	49
R_{HET} [Å]	69
τ_{OF} [ps]	305

[a] R_{HOM} and R_{HET} are the Förster radii for homo- (UPy−OF−UPy → UPy−OF−UPy) and hetero-transfer (UPy−OF−UPy → UPy−OPV), and τ_{OF} is the natural lifetime of UPy−OF−UPy, as obtained from PL decay measurements (see Figure 3). R_{HOM} and R_{HET} were calculated via eq 3, using $\Psi_{OF} = 0.65$,[31] $n = 1.446$, and $\kappa^2 = 4$. The corresponding spectral overlap factors were obtained using eq 4 for the spectra shown in Figure 2.

of an oligo-indenoflorene was calculated to be delocalized across only ~2 of its repeat units.[68] For the calculations presented here, we have therefore used our recently introduced alternative approach based on a modified line-dipole model, which takes into account dynamic self-localization of the excited state.[66] In this model, the geometrically relaxed donor state is taken to be completely localized at the center of the chromophore with a point-dipole transition moment, while the ground state of the acceptor is considered to be completely delocalized as in the line-dipole approach. Equation 6 then simplifies to

$$k_{DA} = \frac{1}{\tau_D}(R_0)^6\left[\sum_j^L \frac{\psi(j)}{R'^3_{DAj}}\right]^2 \quad (7)$$

Here, R'_{DAj} is the distance from the center of the donor to the center of the jth subdipole on the acceptor.

Monte Carlo Algorithm. To model the temporal decay of the photoluminescence from UPy−OF−UPy in the presence of UPy−OPV, a Monte Carlo (MC) algorithm was developed, which describes the random walk of excitations along the chain and to the chain ends. At the beginning of each MC cycle, chains composed of i UPy−OF−UPy units are generated, with i ranging from 1 up to 200 because for the mixing ratios considered here, chain configurations with $i > 200$ are highly unlikely to exist in the distribution. As a first step, the algorithm used a random number generator[69] to select a UPy−OF−UPy site within a chain of configuration i onto which it placed an excitation at time $t = 0$. The transport of the excitation along the chain is then simulated as a random walk in time, which is discretized with a step size of $\Delta t = 1$ ps. Within Δt, the excitation may either transfer to another chromophore within the chain, remain on the current site, or decay radiatively. For a sufficiently small Δt, the probability that energy transfer from site m to site n occurs within Δt is given by $k_{mn}\Delta t$, while the probability for radiative decay is equal to $\tau^{-1}\Delta t$ with τ being the natural decay time of the excitation. The probability for the excitation to remain on site m is then consequently equal to $1 - \Delta t(\tau + \Sigma_{n\neq m}k_{mn})$. The rates k_{mn} were calculated according to eq 7 using the values for a, b, and c given in Table 1 and the experimentally obtained parameters in Table 2. Prior to each MC cycle, the random number generator was used to select from these probability-weighted processes. This procedure is iterated until either the excitation has transferred to an end-capping UPy−OPV site, or until it has decayed, in which case the "emitted" photon is detected.

The probability for an incident photon to be absorbed by a UPy−OF−UPy unit embedded in a chain of configuration i is directly proportional to the effective weight distribution function $w_{eff}(i)$. Therefore, to obtain the intensity decay curves for given x within reasonable time, the trajectories of 300 000 excitations were simulated via the procedure described above, where the contribution from each chain configuration i is weighted according to $w_{eff}(i)$. Thus, a comparative study of the differences in the obtained simulated excitation decay curves for a range of different distribution functions could easily be accomplished.

Supramolecular Chain Polydispersity

In pure dilute solutions of either UPy−OPV−UPy or UPy−OF−UPy, supramolecular chains of great lengths have been shown to form.[15,27] However, viscosity measurements have revealed that addition of small amounts of UPy−OPV reduces the average chain length significantly, as the monofunctional UPy−OPV acts as a chain stopper.[32,33] For an assessment of the chain length distribution in a system of end-capped supramolecular chains, the ultimate test is a comparison of the experimental energy transfer dynamics with curves simulated for potential distribution functions. For this purpose, we have chosen three plausible "test candidates": a derivative of the Flory distribution, a Poisson distribution, and a Delta function. These represent in essence the three scenarios of: equal reactivity of all groups at any stage (step polymerization), addition of new groups to only the chain end (chain polymerization), or the presence of only one chain length (monodispersity), respectively. In the following, we comment on the weight fraction distributions obtained for each case and test their applicability to the supramolecular chain forming process.

Weight Fraction Distribution Functions. Following the approach by Flory,[14] we can derive a weight fraction distribution function on the basis of the assumption of equal reactivity of all functional groups. For such a condensation process into a linear polymer, each functional group of a given chemical nature at every stage of the process carries the same probability to react, independent of the length of the polymer chain to which it is attached. The resulting weight fraction distribution for such a step polymerization process then follows a Flory distribution.[14] The formation of supramolecular polymer chains in the UPy−OF−UPy:UPy−OPV solutions can be treated analogously to a polycondensation process of a monofunctional reactant **R**−**A** (UPy−OPV) and a bifunctional reactant **A**−**R′**−**A** (UPy−OF−UPy). Here, **A** denotes identical functional groups capable of reacting with one another in a reversible addition reaction, and **R** and **R′** stand for nonreactive chemical rest-groups. Thus, upon mixing UPy−OF−UPy and UPy−OPV at a certain ratio x, three different families of chains are expected to form,[70] which have either both ends free, or one end free and the other end-capped by a monofunctional UPy−OPV unit, or both ends end-capped with UPy−OPV. However, Ercolani[70] showed that for very large dimerization constants (as is the case for UPy-groups[15,26]), the latter of these three families represents by far the dominating type of chains in such a blend of mono- and bifunctional reactants; that is, all chains can be considered to be capped on both ends. The concentration $[OF_i]$ of double-end-capped chains composed of i UPy−OF−UPy units can

(67) Tretiak, S.; Saxena, A.; Martin, R. L.; Bishop, A. R. *Phys. Rev. Lett.* **2002**, *89*, 097402.
(68) Beljonne, D.; Hennebicq, E.; Daniel, C.; Herz, L. M.; Silva, C.; Scholes, G. D.; Hoeben, F. J. M.; Jonkheijm, P.; Schenning, A. P. H. J.; Meskers, S. C. J.; Phillips, R. T.; Friend, R. H.; Meijer, E. W. *J. Phys. Chem. B* **2005**, *109*, 10594.
(69) Press, W. H.; Teukolsky, S. A.; Vetterling, W. T. *Numerical Recipes in C: The Art of Scientific Computing*; Cambridge University Press: Cambridge, 1993.
(70) Ercolani, G. *Chem. Commun.* **2001**, 1416.

consequently be derived as (for details, see the Supporting Information):

$$[\mathrm{OF}_i] = 2^{i-1}x^2(2+x)^{-(i+1)}[\mathrm{OF}]_0 \quad (8)$$

Here, $[\mathrm{OF}]_0$ denotes the concentration of UPy−OF−UPy molecules, and the mixing ratio x is defined as the ratio between the concentrations of UPy−OPV and UPy−OF−UPy units, that is, $x = [\mathrm{OPV}]_0/[\mathrm{OF}]_0$. Note that the special case of $i = 0$ corresponds to the situation where two end-caps hydrogen bond to form a short chain that contains no UPy−OF−UPy molecules.

To replicate the photoemission of the chain ensemble in the solution, the most useful input to the simulations is the weight fraction distribution function $w_{\mathrm{eff}}(i)$, which gives the probability of finding a UPy−OF−UPy unit as part of a chain of length i within the distribution. $w_{\mathrm{eff}}(i)$ is directly related to the concentrations of chains and UPy−OF−UPy units through

$$w_{\mathrm{eff}}(i) = \frac{i[\mathrm{OF}_i]}{[\mathrm{OF}]_0} \quad (9)$$

Inserting eq 8 yields:

$$w_{\mathrm{eff}}(i) = i2^{i-1}x^2(2+x)^{-(i+1)} \quad (10)$$

Thus, the weight fraction distribution is solely a function of the mixing ratio, which is an externally controllable variable.

An alternative approach can be taken by assuming that growth of the supramolecular chains occurs in such a way that monomers are only added to the active group at the chain end, and subsequently form the new end.[14,16] Such chain polymerization processes differ from the step-polymerization growth mechanism described by the Flory distribution (eq 10) for which groups already linked together can yet again be coupled with other groups. For chain polymerization, the resulting weight distribution function is typically much narrower than in the case of step polymerization and can be described as a Poisson distribution.[14,16] Assuming again an absence of unsaturated UPy-groups present in the sample, and expressing the mean chain length as $(2)/(x)$, one arrives at the following expression for the relative concentrations:

$$[\mathrm{OF}_i] = \frac{\left(\frac{2}{x}\right)^i}{i!}e^{-2/x}[\mathrm{OF}]_0 \quad (11)$$

According to eq 9, the weight distribution function is then given by:

$$w_{\mathrm{eff}}(i,x) = \frac{\left(\frac{2}{x}\right)^i}{(i-1)!}e^{-2/x} \quad (12)$$

Finally, a third approach is based on the simplified assumption of a monodisperse chain distribution. Drain et al. recently suggested that in a blend of chain building and stopping reactants, there is a predominance of the chain configuration given by the stochiometric ratio between the two species.[25] This assumption implies essentially that for a given mixing ratio x, only chains composed of $(2)/(x)$ UPy−OF−UPy units are formed, while the concentration of chains of different configuration remains negligible. Following this intuitive approach, one can describe the concentration $[\mathrm{OF}_i]$ of chains composed of i UPy−OF−UPy units by using Kronecker's δ-function, that is:

$$[\mathrm{OF}_i] = \frac{x}{2}\delta\left(i - \frac{2}{x}\right)[\mathrm{OF}]_0 \quad (13)$$

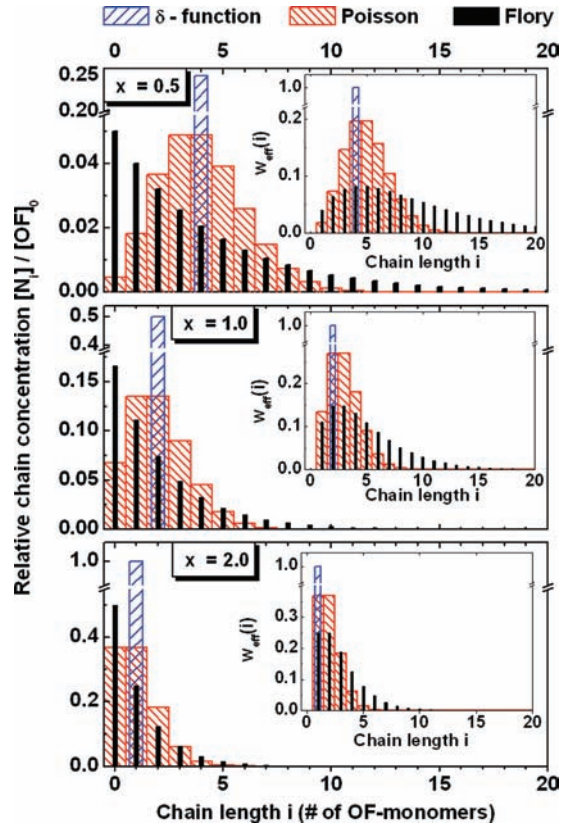

Figure 5. Concentration $[\mathrm{OF}_i]$ of chains containing i UPy−OF−UPy units, normalized by the overall concentration $[\mathrm{OF}]_0$ of UPy−OF−UPy molecules in the solution, against i for three different distribution functions and mixing ratios. The insets show the corresponding effective weight fractions w_{eff} of the chains of configuration OF_i against their polymerization degree i.

Consequently, the effective weight function w_{eff} is given by

$$w_{\mathrm{eff}}(i,x) = \delta\left(i - \frac{2}{x}\right) \quad (14)$$

Figure 5 allows a comparison between the three different chain distributions for a number of mixing ratios x. The relative chain concentration $[\mathrm{OF}_i]/[\mathrm{OF}]_0$ shows distinct differences between these cases. For the Flory distribution, the $[\mathrm{OF}_i]$ number distribution decreases monotonically in chain length i, with chains merely composed of two UPy−OPV units ($i = 0$) always exhibiting the highest concentration. In contrast, for both the Poisson and the δ distribution, chains with mean chain length $(2)/(x)$ have the highest concentration in the ensemble. The effective weight distribution function w_{eff} (shown in insets to Figure 5) is zero for $i = 0$ in all three cases as the probability of finding an UPy−OF−UPy unit in a UPy−OPV dimer is zero. Importantly, w_{eff} is much broader for the Flory than for the Poisson distribution, with longer chains making a significantly higher contribution in the former case.

Comparison between Experiment and MC Simulations. The three different chain weight distribution functions were alternately used as input into the MC simulation to generate theoretical predictions for the decay of the UPy−OF−UPy emission in the presence of UPy−OPV. Figure 6 shows the simulated decay curves obtained for the three distribution functions together with the experimental data. It can be clearly seen that the choice of chain distribution function has a profound effect on the simulated donor emission transients, with strong discrepancies in the predicted shapes of the transients becoming

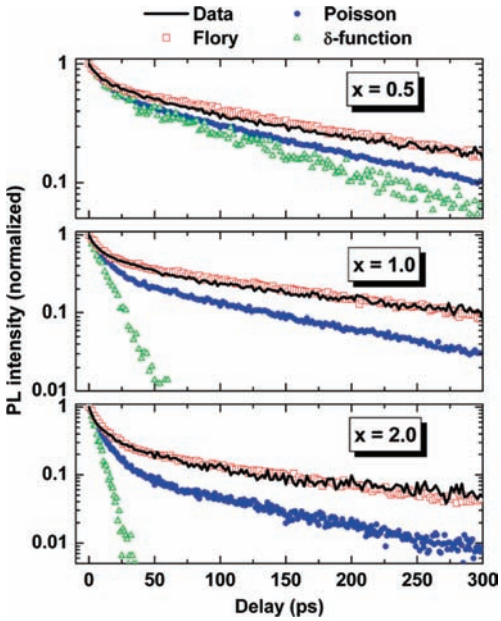

Figure 6. Comparison between experimental time-resolved PL intensity data and simulations at varying mixing ratios, where the polydispersity of the supramolecular chains has been modeled with various distribution functions.

particularly evident at high mixing ratios x. This effect arises because isolated transients for each individual chain composition differ substantially from one another depending on chain length, with fast decay components arising from short chains and long components from lifetime-limited decays on long chains. The weighting of short- to long-decay components in the transient therefore directly maps out the prevalence of short to long chains in the ensemble. For this reason, modeling the energy transfer dynamics along these chains and to the chain ends is a powerful way of assessing the chain weight distribution function for a supramolecular polymer ensemble.

Comparison of the simulated decay curves with the experimental data shows excellent correspondence with the assumption of a Flory distribution of chain lengths, with full overlap between data and simulation over all measured blend ratios x. The Poisson distribution clearly does not provide an adequate description of the real chain distribution because it underestimates the presence of long chains in the ensemble, as discussed above. Finally, the assumption of a monodisperse ensemble as described by the Delta-function distribution, while intuitively satisfying, leads to a poor match between simulated and experimental donor decay transients. In particular, for very short chains containing only one or two UPy−OF−UPy units ($x = 2$ or 1), a single-exponential decay is predicted by the simulation, which clearly bears little resemblance to the data. This effect again arises from the neglect of long chains in the ensemble for a Delta-like chain weight distribution, as shown in Figure 5.

To assess the influence of variations on the determined geometrical structure of the system, the previous simulations were repeated under variation of each of the structural parameters a, b, and c. Exemplary results for one mixing ratio are shown in Figure 7. It is apparent that the simulations show much stronger sensitivity toward the choice of chain weight distribution function than toward changes in the structural parameters. Even for relatively large changes of ∼10% in a, b, and c, which fall outside the reasonable error in the determination of these parameters, a good match between data and simulation is obtained for the Flory distribution, while the Poisson and Delta function provide an inadequate description.

Our assessment yields unambiguous evidence for the Flory distribution providing the correct description of the chain length distribution in an ensemble of supramolecular polymer chains terminated with end-stoppers. These results demonstrate that the formation of supramolecular polymers follows a step-polymerization reaction with equal reactivity of all supramolecular building blocks at any stage. "Growth" of the supramolecular chain is therefore a dynamic process involving all chain

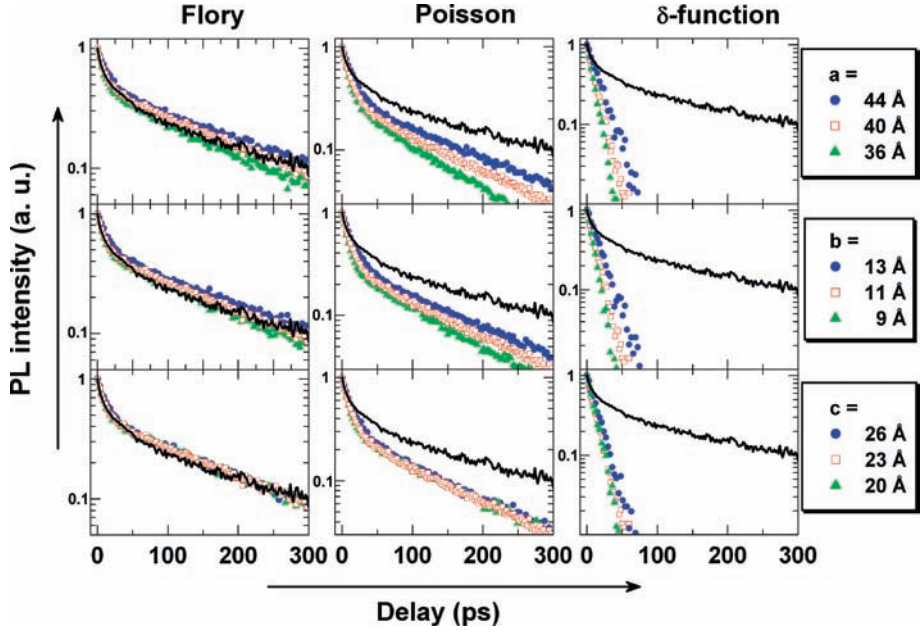

Figure 7. The dependency of the simulated PL decay curves on the numerical values of the structural parameter values is shown for various distribution functions at a fixed mixing ratio of $x = 1.0$. Each of the three structural parameters is varied individually by approximately ±10% from the calculated values given in Table 1, while the remaining parameters are kept constant. For comparison, the experimental data obtained for $x = 1.0$ are displayed (black, solid line) in all graphs.

components at all times. It thus cannot be adequately described by the chain polymerization processes typical for some synthetic procedures that covalently link monomers from the chain end onward into a fully conjugated polymer. In addition, the resulting presence of a large number of long supramolecular chains means that the distribution function for the ensemble is too broad to be approximated as monodisperse.

Conclusion

In the study presented, we have investigated the formation process of supramolecular linear polymer chains and its influence on the resulting chain length distribution function. For this purpose, we explored the migration of excitation energy along the main chain comprising units of bifunctional UPy−OF−UPy and to the chain ends of monofunctional UPy−OPV acting as excitation traps. Using time-resolved PL spectroscopy, the emission emerging from UPy−OF−UPy in blend solutions of both compounds was found to suffer from dynamic quenching, which increased with the concentration of UPy−OPV in solution. This finding provides evidence for efficient energy transfer from UPy−OF−UPy to UPy−OPV units, in accordance with strong spectral overlap between photon emission of the former and absorption by the latter.

The experimentally obtained decay transients were subsequently modeled using a Monte Carlo algorithm that reproduced the UPy−OF−UPy emission in the presence of UPy−OPV for a given mixing ratio. For these simulations, the electronic donor−acceptor coupling was calculated using a modified line-dipole approach,[66] which takes into account the localized character of the relaxed excited state.[67] Structural parameters to describe the extent of the π-conjugated systems and the hydrogen-bonded UPy bridge were extracted from molecular modeling based on the semiempirical Austin Model and used as input parameters to the simulation. The simulations were run on ensembles of chains generated from three different weight distribution functions to be tested: a derivative of the Flory distribution,[14,70] a Poisson distribution, and, finally, a Delta function representing the case of a monodisperse sample. As a result of the well-defined geometries of both the oligomers used and the supramolecular chains, these served as an ideal model system, requiring few input parameters and therefore permitting an accurate assessment of the polymer weight function distribution from a comparison between data and simulation.

The choice of chain distribution function was found to have a strong effect on the shapes of the simulated PL decay transients. This effect is caused by the excitation transfer rate from the main chain to the chain end depending crucially on the distance of the originally created excitation from the chain ends. As a result, fast initial decay components are generated by the presence of short chains, while lifetime-limited decays reflect the presence of relatively long chains. The distribution of chains in the ensemble thus shows a direct correspondence with the observable distribution of transfer rates that is represented in the overall decay transient. Therefore, a comparison between experimental and simulated excitation transfer dynamics is a powerful approach toward determining the chain weight distribution function for the supramolecular polymer ensemble.

For the assumption of a Flory distribution of chain lengths, excellent agreement between experimental and simulated data was found over a wide range of mixing ratios. On the other hand, the Poisson distribution clearly underestimated the presence of relatively long chains in the ensemble. Particularly poor matches between simulation and data were obtained for the strongly simplified assumption of a monodisperse sample. The distinction between Flory and Poisson distribution functions is of particular interest because these are the result of two profoundly different growth mechanisms during polymerization, with the former representing a step-polymerization process, equivalent to polycondensation of linear covalent polymers, and the latter a chain-polymerization with growth occurring from the chain ends only. Our results therefore clearly show that equal reactivity of the supramolecular building blocks leads to a dynamic growth process for the supramolecular chain involving all chain components at all times. These findings are important for the understanding of reversible polymerization processes, as they represent an experimental verification of so far only theoretically derived weight fraction distribution functions. Such knowledge of both structure and polydispersity of chains is crucial for the application of supramolecular polymers in molecular electronics.[15]

Acknowledgment. Financial support for this work was provided by the Engineering and Physical Sciences Research Council (UK).

Supporting Information Available: Details of the derivation of the weight fraction distribution given in eq 10. This material is available free of charge via the Internet at http://pubs.acs.org.

JA9080452